Study On Marine Boundary Layer Aerosol Structure based on Satellite Observations

Shumei Deng [1,2,a], Mingjian Yi [1,2,b], Qiang Zhao [1,2,c], Changyu Liu [1,2,d]

[1] School of Environment and Energy Engineering, Anhui Jianzhu University, Hefei, Anhui, 230031, China

[2] Key Laboratory of Huizhou Architecture in Anhui Province, Hefei, Anhui, 230031, China

[a] dsmltlmy@163.com, [b] mjyi@ustc.edu.cn, [c] rommel99@163.com, [d] 1043941348@qq.com

Abstract. The aerosol vertical distribution in the boundary layer is heavily influenced by the boundary layer thermal structure. This paper studied on marine boundary layer (MBL) aerosol and its structure by using satellite lidar measurements. The lidar methodology was improved and applied to the 3-year satellite MBL aerosol observations over Oceans, and a new global ocean dataset was built. The global MBL structure were examined and discussed with the new dataset. Results showed that the BLH generally increases and MLH generally decreases when away from the coast. Further analyze shows that the MBL tends to be more well-mixed with lower BLH, and the aerosol loading shows weaker relationships with U10m under overcast conditions than partly cloudy conditions. This study demonstrated that satellite lidar measurements have the great potential in evaluating and constraining both modeled MBL aerosol optical properties and modeled MBL structure.

Keywords: Marine boundary layer; Aerosol structure; Satellite observation.

1. Introduction

Sea salt is one of the largest natural contributors to the global aerosol loading. Sea salt dominates sub- and super- micron scatterers in most oceanic regions and the marine boundary layer (MBL) particulate mass concentration in remote oceanic regions [1]. Sea salt also serves as the dominant source of cloud condensation nuclei over the remote oceanic regions, and thus can affect radiative budget by indirect-radiative-effect [2-4].

Despite of its significant role in the global climate, sea salt aerosol is still one of the most poorly constrained aerosols in models [5-6]. The large differences among different models could result in large uncertainties in corresponding radiative forcing estimations [7-12].

The aerosol vertical distribution in the boundary layer is heavily influenced by the boundary layer thermal structure. Meanwhile, the representation of convection and MBL processes are also critical to the successful simulations of climate in many other aspects, such as marine low cloud [13-14]. Due to the close connection between MBL aerosol and MBL-related processes, 3-year satellite measurements will be used to study the MBL aerosol structure over Oceans, by taking the advantages of The Cloud-Aerosol Lidar with Orthogonal Polarization (CALIOP). Section 2 introduces the dataset used in this paper. Section 3 presents the new global MBL structure datasets and analyzed the MBL structure under different conditions. Conclusions and discussions are given in Section 4.

2. Dataset

Multiple remotely sensed datasets over Oceans during the period of Jan. 2007 to Dec. 2009 are used in this study.

CALIOP, carried on Cloud-Aerosol Lidar and Infrared Pathfinder Satellite Observations (CALIPSO), is a unique tool to provide global height-resolved aerosol optical properties [15]. CALIOP level 1B data provides three calibrated and geolocated lidar profiles, which are 532nm and 1064nm total attenuated backscatter and 532nm perpendicular polarization component, with along-track footprint of 333m and the vertical resolution of 30m below 8.2 km. The cloud-free CALIOP measured aerosol backscattering was used to retrieve sea salt aerosol information and identify the MBL structure.

The cloud information, including cloud mask, cloud top height and cloud type, was obtained from the 2B-CLDCLASS-LIDAR [16], which combines CloudSat and CALIOP observations to better identify the cloud boundaries.

The European Center for Medium range Weather Forecasting AUX-algorithm (ECMWF-AUX) [17] provides the temperature and pressure profile, which are used to estimate the molecular backscattering.

AMSR-E Level 3 daily Ocean Products version-5 provides surface wind speed at 10m (U10m), which was produced by Remote Sensing Systems (RSS, http://www.remss.com/).

3. Results

3.1 Construction of global MBL structure datasets

The aerosol layer identification and sea salt extinction retrieval method are the same as detailed in [18]. After identifying the aerosol layer with an improved threshold method to overcome the lower signal-to-noise ratio issue in the space-borne lidar, several criteria were applied to identify the clean marine aerosol cases, and extinction was retrieved by forward iteration method with a lidar ratio of 25.

With the retrieved MBL aerosol extinction profiles, the derived aerosol layer top height can be a good proxy for the marine boundary layer height (BLH), and the mixing layer height (MLH) can be identified with the gradient method [19]. As evaluated with the ground-based lidar and radio sound observations, the bias and root-mean-square (RMS) difference of lidar-derived BLH is -0.12±0.24km [19]. Evaluations with the MAGIC sounding observations showed that the bias and RMS difference in CALIOP-derived BLH is -0.14±0.37 km, and -0.1±0.45 km in MLH [20].

As stated above, the clear-sky BLH can be estimated from the MBL aerosol layer top by the threshold method. For cloudy-sky, the BLH can be estimated from the marine stratiform cloud top, which is a good proxy to estimate marine BLH under cloudy conditions as widely used in the previous studies [21-22]. Therefore, combing these two, all sky BLH can be estimated. Figure 1 shows the so-derived global distributions of mean BLH (Fig. 1(a)) and MLH (Fig. 1(b)) from satellite observations. As shown in the Fig, the BLH generally increases and MLH generally decreases when away from the coast, corresponding with the regions transiting from stratiform clouds (Scs) to cumulus clouds (Cus), which also indicates the decreasing atmospheric stratification.

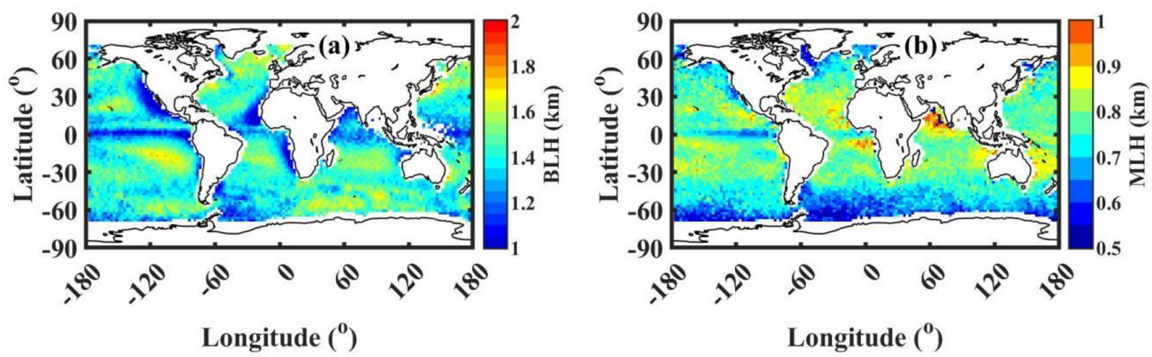

Fig. 1. Global distribution of mean MBL structure. (a) BLH; (b) MLH.

3.2 MBL vertical structure characteristics

Figure 2 shows the retrieved mean MBL aerosol extinction profiles under different U10m and BLH bins and different low cloud fraction (LCF) conditions. Though the observed aerosol extinction was observed only under clear-sky conditions, for each collocated case, the observation was divided into two categories, that is, clear or partly cloudy condition with LCF < 0.3 in the same 25km collocated grid box, and overcast condition with LCF > 0.5 in the same 25km collocated grid box. The MBL structure could be less affected by the cloud under partly cloudy condition, and it is assumed that the cloud-topped MBL can have the similar structure to the nearby clear-sky MBL within the 25km footprint under overcast condition.

Under the partly cloudy condition, when BLH is lower than 1km or U10m < ~6 m/s, it can be observed that sharper gradient in extinction can be found near the top of the observed aerosol layer than other part of the aerosol layer. The observed aerosol layer tends to be better mixed especially BLH is lower than 1km. When BLH is higher than 1km and U10m > ~6 m/s, the observed MBL aerosol layer shows decoupled structure, with a lower well-mixed layer and an upper decouple layer. It should be noted that those cases with BLH higher than 1km and U10m > ~6 m/s mostly happen over the Sc-to-Cu transition regions. The MBL characteristics under overcast conditions are generally similar to those under partly cloudy conditions, except that the aerosol loading shows weaker relationships with U10m. Wind shear is the main driven factor of sea salt aerosol source. Weaker relationships between aerosol loading and U10m under overcast conditions indicates that other processes, i.e. drizzle, may play important role.

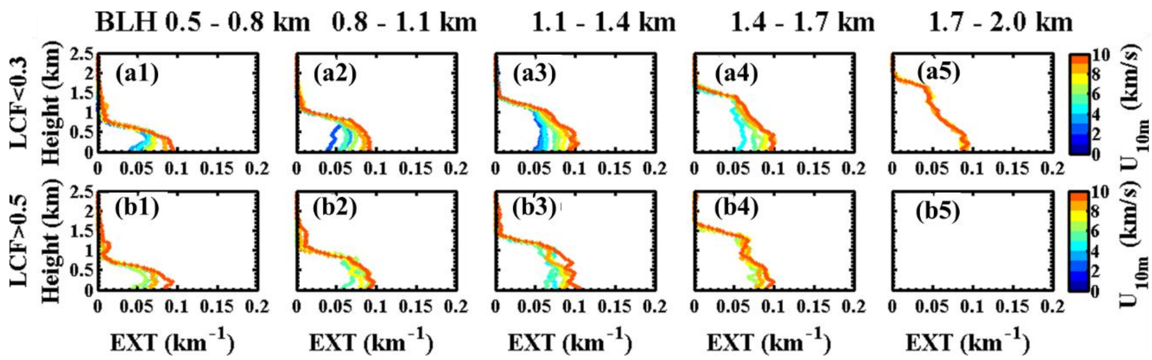

Fig. 2. mean aerosol extinction profiles under different U10m and BLH bins and different (low cloud fraction) LCF conditions. The LCF in observation is defined as the LCF in each 25 km footprint.

4. Conclusion and discussion

Due to the close connection between MBL aerosol and MBL processes, the aerosol information could be a good proxy to determine the MBL structure. The lidar methodology was improved and applied to the 3-year satellite MBL aerosol observations over Oceans, and a new global ocean dataset was built. The global MBL structure were examined and discussed with the new dataset. Results showed that the BLH generally increases and MLH generally decreases when away from the coast. Further analyze shows that the MBL tends to be more well-mixed with lower BLH, and the aerosol loading shows weaker relationships with U10m under overcast conditions than partly cloudy conditions.

This study demonstrated that satellite lidar measurements offer a unique opportunity to characterize MBL and has great potential in constrain both modeled MBL aerosol optical properties and modeled MBL processes. Our further step is to improve the modeled MBL processes with the satellite lidar observations in our future work.

References

[1] Sievering H, Cainey J, Harvey M. et al. Aerosol non-sea-salt sulfate in the remote marine boundary layer under clear-sky and normal cloudiness conditions: Ocean-derived biogenic alkalinity enhances sea-salt sulfate production by ozone oxidation, J. Geophys. Res., 2004, 109.

[2] Albrecht B A. Aerosols, cloud microphysics, and fractional cloudiness, Science, 1989, 245, 1227-1230.

[3] Twomey, S. Pollution and the planetary albedo, Atmos. Environ., 1974, 8, 1251-1256.

[4] Twomey, S. The influence of pollution on the shortwave albedo of clouds, J. Atmos. Sci., 1977, 34, 1149-1152.

[5] Textor C, Schulz M, Guibert S, et al., Analysis and quantification of the diversities of aerosol life cycles within AEROCOM, Atmospheric Chemistry and Physics, 2006, 6, 1777-1813.

[6] Kinne S, Schulz M, Textor C, et al. An AeroCom initial assessment – optical properties in aerosol component modules of global models, Atmos Chem Phys, 2006, 6, 1815-1834.

[7] Winter B, and Chylek P. Contribution of sea salt aerosol to the planetary clear-sky albedo, Tellus B, 1977,49, 72-79.

[8] Haywood, J M, Ramaswamy V, and Soden B J. Tropospheric aerosol climate forcing in clear-sky satellite observations over the oceans, Science, 1999, 283, 1299-1303.

[9] Jacobson, M Z. Global direct radiative forcing due to multicomponent anthropogenic and natural aerosols, J. Geophys. Res., 2001, 106, 1551-1568

[10] Grini, A, Myhre G, Sundet J K, and Isaksen I S A. Modeling the annual cycle of sea salt in the global 3-D model Oslo CTM2: Concentrations, fluxes, and radiative impact, J. Climate, 2002, 15, 1717-1730.

[11] Ayash T, Gong S, and Jia C Q. Direct and indirect shortwave radiative effects of sea salt aerosols, J. Climate, 2008, 21, 3207-3220.

[12] Ma X, Salzen K, and Li J. Modelling sea salt aerosol and its direct and indirect effects on climate, Atmos. Chem. Phys., 2008, 8, 1311-1327.

[13] Stull R B and Eloranta E W. Boundary layer experiment 1983, Bull. Am. Meteorol. Soc., 1984, 65, 450-456.

[14] Leventidou E, Zanis P, Balis D, et al. Factors affecting the comparisons of planetary boundary layer height retrievals from CALIPSO, ECMWF and radiosondes over Thessaloniki, Greece. Atmospheric Environment, 2013, 74, 360-366.

[15] Winker D M, Hunt W H, and McGill M J. Initial performance assessment of CALIOP, Geophys. Res. Lett., 2007, 34, L19803, doi:10.1029/2007GL030135.

[16] Wang, Z. Level 2 Combined Radar and Lidar Cloud Scenario Classification Product Process Description and Interface Control Document. 2013.

[17] Partain, P. Cloudsat ECMWF-AUX Auxiliary Data Process Description and Interface Control Document, 2004.

[18] Luo T, Yuan R., and Wang Z. On Factors Controlling Marine Boundary Layer Aerosol Optical Depth. J. Geophys. Res., 2014, 119.6: 3321-3334.

[19] Luo T., R. Yuan, and Z. Wang. Lidar-based Remote Sensing of Atmospheric Boundary Layer Height over Land and Ocean. Atmospheric Measurement Techniques. 2014, 7, 1: 173-182.

[20] Luo T., R. Yuan, Z. Wang, and D. Zhang. Quantifying the Hygroscopic Growth of Marine Boundary Layer Aerosols by Satellite-Based and Buoy Observations. J. Atmos. Sci., 2015, 72, 1063-1074.

[21] Wood R and Bretherton C S. Boundary Layer Depth, Entrainment, and Decoupling in the Cloud-Capped Subtropical and Tropical Marine Boundary Layer, J. Climate, 2004, 17, 3576-3588.

[22] Zuidema, P, Painemal D, Szoeke S de, Fairall C. Stratocumulus Cloud-Top Height Estimates and Their Climatic Implications, J. Climate, 2009, 22, 4652-4666.